Republic of Kazakhstan. Series of Geology and Engineering Sciences. 2020. Vol. 4, No. 442. pp. 62–69.
3. Tsoi S. V., Oryngozhin E. S., Metaksa G. P., Zhangalieva M. Zh., Alisheva Zh. N. et al. Evaluation of existing technology and development of an alternative method for the exploitation of hydrogenous uranium deposits. *International Conference on Actual Achievements of European science*. Sofia, Bulgaria, 2018. pp. 40–44.
4. Bitimbayev M. Zh., Krupnik L. A., Aben Kh. Kh., Aben E. Kh. Adjustment of backfill composition for mineral mining under open pit bottom. *Gornyi Zhurnal*. 2017. No. 2. pp. 57–61.
5. Krupnik L. A., Bitimbayev M. Zh., Shaposhnik S. N., Shaposhnik Y. N. et al. Validation of rational backfill technology for Sekisovskoe deposit. *Journal of Mining Science*. 2015. Vol. 51, No. 3. pp. 522–528.
6. Oryngozha Ye. Ye., Vorobiev A. Ye., Zhangalieva M., Uteshev I. Zh. Study of mining-geological characteristics of uranium deposits in Kazakhstan for development by in-situ leaching. *News of the National Academy of Sciences of the Republic of Kazakhstan. Series of Geology and Engineering Sciences*. 2020. Vol. 5, No. 443. pp. 156–164.
7. Vorobev A. Y., Metaxa G. P., Bolenov Y. M., Metaxa A. S., Alisheva Z. N. Digitization of the mining industry. Concept and modern geotechnology. *News of the National Academy of Sciences of the Republic of Kazakhstan. Series of Geology and Engineering Sciences*. 2019. Vol. 4, No. 436. pp. 121–127.
8. Lewandowski K. A., Kawatra S. K. Binders for heap leaching agglomeration. *Minerals and Metallurgical Processing*. 2009. Vol. 26, No. 1. pp. 1–24.
9. McNab B., Crushing L. Exploring HPGR Technology for Heap Leaching of Fresh Rock Gold Ores. *IIR Crushing & Grinding Conference*. Townsville. Australia, 2006.
10. Moldabayeva G. Z., Metaxa G. P., Alisheva Z. N. Theoretical bases for the implementation of the processes to reduce viscosity in the conditions of natural reservation. *News of the National Academy of Sciences of the Republic of Kazakhstan. Series of Geology and Engineering Sciences*. 2019. Vol. 5, No. 437. pp. 138–143.
11. Malkova M. Yu., Zadiranov A. N. Application of the universal ultrasonic reactor in the processing of rare earth metal ores concentrates. *RUDN Journal of Engineering Researches*. 2019. Vol. 20, No. 1. pp. 20–27.
12. Toraman O. Y. Experimental investigations of preparation of calcite particles by ultrasonic treatment. *Physicochemical Problems of Mineral Processing*. 2017. Vol. 53, No. 2. pp. 859–868.
13. Mullakaev M. S. Ultrasonic intensification of the processes of enhanced oil recovery, processing of crude oil and oil sludge, purification of oil-contaminated water. Moscow : HELRI, 2018. 376 p.
14. Sinusoidal vibroviscometer. User's Guide. A&D Company, Limited, 2017. 56 p.
15. Xu Y., Langbauer C., Hofstaetter H. The Application of Ultrasonic Technology for Cleaning Oil Contaminated Sand. *SPE Asia Pacific Health, Safety, Security. Environment and Social Responsibility Conference*. Kuala Lumpur, 2017. DOI: 10.2118/185261-MS
16. Amirova U. K., Uruzbaeva N. A. Overview of the world market of uranium. *Universum: ekonomica i yurisprudentsiya*. 2017. No. 6(39).
17. Kundu T. Nonlinear Ultrasonic and Vibro-Acoustical Techniques for Nondestructive Evaluation. Springer International Publishing. 2019. 759 p. DOI: 10.1007/978-3-319-94476-0
18. Hirao M., Ogi H. Electromagnetic Acoustic Transducers: Noncontacting Ultrasonic Measurements Using EMATs. Japan : Springer Tokyo, 2017. 382 p. DOI: 10.1007/978-4-431-56036-4 EM

UDC 622.7:622.341.11

T. N. GZOGYAN[1], *Head of Laboratory*
S. R. GZOGYAN[1], *Senior Researcher, mehanobr1@yandex.ru*
E. V. GRISHKINA[1], *Researcher*

[1] *Belgorod State University, Belgorod, Russia*

PROCESSING TECHNOLOGY FOR FERRUGINOUS QUARTZITE OF OKOLOVO DEPOSIT

The article describes mineralogical and technological studies of ferruginous quartzite of Okolovo deposit. A signature of the mineral composition of ferruginous quartzite from this deposit is a noticeable predominance and diversity of silicate minerals as against quartz. The presence of low metallic and nonmetallic materials in quartzite dictates their extraction in the process of ore pretreatment.

The promising trend in processing of ferruginous quartzite of Okolovo deposit is combination of pretreatment and deep concentration. The technological research has proved feasibility of obtaining a high-quality product suitable for metallization using the recommended technology.

Keywords: *ferruginous quartzite, magnetite, hematite, martite, quartz, dry magnetic separation, wet magnetic separation, grindability*

DOI: *10.17580/em.2023.01.10*

Introduction

Ferruginous quartzite of Okolovo deposit is a promising source of raw materials for mining and processing. The commercial reserves are estimated as 145.4 Mt at the contents of $Fe_{magnetic} = 8.0–26.1\%$ and $Fe_{total} = 15.0–31.7\%$. In terms of processability, ferruginous quartzite belongs to the categories of readily grindable and easy minerals [1]. The deposit is composed of 11 sheet-like ore bodies of variable thickness, with feathering-out or thin schistocity, and with replacement of ferruginous quartzite by gangue with magnetite pockets both along and across the strike. The deposit has a characteristic two-level structure: the crystalline basement is overlaid with a thick cover of igneous-sedimentary and sedimentary rocks. The cover is composed of the Upper Proterozoic and Meso-Cenozoic strata. Three layers of ferruginous quartzite (from 20–80 to 125–260 m thick) feature a monoclinal bedding with the southeastward dip at 60–80° and contain up to 5–6 ore beds each [2]. The base minerals are silica-and-magnetite quartzite and magnetite amphiboles. Alongside with these base mineralogical and petrographic varieties, there is a little magnetite–biotite, magnetite–pyroxene and semi-oxidized quartzite. The basic metallic mineral is magnetite; sometimes iron sulfides (pyrite, pyrrhotine and chalcopyrite) and ilmenite, as well as martite, hematite and limonite (in the underdeveloped oxidation zone) are observed. The average content of Fe_{total} in the pay zones is 27.0% [1, 2].

The main objective of this study is to develop an optimal technology to manufacture an iron product suitable for the metallization.

Technological research

The test objects were the bulk core samples (1.33 t) from two ore bodies (samples Nos. 1 and 2—ore body 1; sample No. 3—ore body 2; sample No. 4—mix of ferruginous quartzite from both ore bodies) represented in full the texture, structure and mineralogy of the test mineral. The research methodology is described in [3–5].

The chemical and mineral compositions, and the Fe_{total} distribution are described in **Tables 1** and **2**. The spectral analysis shows the presence of nickel, copper, zinc, cobalt, chrome, lead, vanadium and other elements in all test samples. Ferruginous quartzite under analysis features the low content of both Fe_{total} and Fe_{magn}. The base metallic mineral is magnetite at the content ranged from 16.2 to 23.13%. Magnetite represented by coarse grains and aggregates of polygonal shape composes thin independent interlayers. Furthermore, magnetite is present as single isometric grains and small aggregates in mixed interlayers, and as fine isometric or roundish grains in nonmetallic interlayers. It is observed that magnetite grains and aggregates contain submicron shots of sulfide and nonmetallic minerals, but it is more often that submicron magnetite shots are present in quartz and silicates.

Suboxidized varieties feature the first- and medium-level oxidation with magnetite replacement by martite, sometimes in full, which is confirmed by the magnetite nonuniformity coefficient (0.47–0.55). Martite occurs as a thin hem of magnetite grains, as strings in microcracks and as fine irregular shots in magnetite. Limited iron hydroxides develop both in magnetite and in nonmetallic minerals. Some few hematite plates are observed in metallic interlayers.

The base rock-forming minerals of this deposit are the silicate minerals having the markedly various compositions—garnet, hornblende, cummingtonite, biotite, clinopyroxene, and a little chlorite, epidote and actinolite. Silicate minerals usually compose monomineral nonmetallic interlayers, sometimes together with quartz. The mixed and metallic interlayers also contain silicates. They are typically present as submicron nests in magnetite, which conditions their entry in the concentrate of magnetic separation.

Quartz is one of the most common nonmetallic minerals, it composes monomineral interlayers and also occurs in nonmetallic, mixed and metallic interlayers. The grains of quartz are 0.1–0.4 mm in sizes, and reach the size of 0.5–1.5 mm in monomineral interlayers.

The interlayers of all types contain irregular grains and small nests of carbonates (mostly calcite) as a fill in voids and in diagonal joints.

Table 1. Chemical composition of samples

Compounds and oxides	Content per sample, %			
	No. 1	No. 2	No. 3	No. 4
Fe_{total}	21.720	26.84	27.40	23.67
FeO	14.700	16.62	18.55	17.00
Fe_2O_3	14.740	19.90	18.56	14.90
SiO_2	51.700	48.10	46.50	51.20
Al_2O_3	6.000	5.26	5.14	5.80
CaO	5.880	3.62	5.22	4.98
MgO	2.800	3.10	3.10	3.40
TiO_2	0.200	0.18	0.20	0.25
MnO	0.040	0.11	0.05	0.05
S_{total}	0.073	0.12	0.14	0.13
P_2O_5	0.170	0.19	0.19	0.15
Loss in calcination	1.540	1.70	1.70	1.50
K_2O	0.350	0.53	0.32	0.28
Na_2O	1.440	1.03	1.12	1.12
Fe_{magn}	11.730	16.75	15.48	12.15
Coefficient of: magnetite nonuniformity ash content alkalinity	 0.500 33.610 82.410	 0.55 44.71 58.12	 0.50 51.09 52.55	 0.47 54.92 59.15

The thin independent interlayers are formed by fine (to 0.2 mm) isometric grains of apatite.

Sulfides occur mostly as submicron shots of pyrite and pyrrhotine in magnetite, or sometimes as single grains and small nests, or fill in diagonal joints.

The mineralogical research shows that quartzite features an alternation of interlayers of different mineral compositions and with vague interfaces. The texture is often an indistinct lamination of ore interlayers of inconsistent thickness. The medium-laminated structure is composed of interlayers having the average thickness of 3.6–4.6 mm. Regarding linear thickness of interlayers, the metallic interlayers have the smallest thickness (1.4–2.3 mm), and the mixed and nonmetallic interlayers are 3.8–5.4 mm and 3.2–5.2 mm thick, respectively.

The metallic interlayers are composed of coarse grains and irregular aggregates of magnetite; the aggregates are either solid, ribbon–discontinuous or coarse grain–clots. The grains and aggregates of magnetite are often split into blocks by micro joints; sometimes inter-grain and intra-grain jointing is observed. The grains and aggregates of magnetite in the metallic interlayers reach the average size of 0.0782–0.079 mm.

The polygonal grains of magnetite are closely associated with the silicate minerals and quartz in the mixed type interlayers, and occur as single grains and disseminated aggregates in the nonmetallic interlayers. These magnetite grains and aggregates have smaller sizes (0.0523–0.0566 mm).

The nonmetallic interlayers are mostly composed of the silicate minerals with rare submicron shots of magnetite and quartz, and have a grano nematoblastic and grano lepidoblastic structure. The interlayers are seldom composed of mosaic quartz with single submicron shots of magnetite and silicates.

Physically, quartzite has a medium and low strength which is proved by the hardness factor on Protodyakonov's scale (3.11–7.56) and by the specific energy to failure (1.12–7.0 kg·m/cm^3). Rarely the hardness factor reaches 12.0 (magnetite–hornblende variety) and

Table 2. Mineral composition of test samples

Mineral	Content of minerals (M) and total iron per sample, %							
	No. 1		No. 2		No. 3		No. 4	
	M	Fe_{total}	M	Fe_{total}	M	Fe_{total}	M	Fe_{total}
Magnetite	16.20	11.73	23.13	16.75	21.38	15.48	16.78	12.15
Martite+hematite	0.75	0.52	2.81	1.97	2.11	1.48	0.61	0.13
Silicates	55.90	9.40	47.03	8.00	53.09	10.27	55.00	10.94
Carbonates	1.56	-	1.70	-	1.45	-	1.37	-
Sulfides	0.16	0.07	0.25	0.12	0.32	0.17	0.30	0.15
Quartz	25.03	-	24.63	-	21.2	-	25.57	-
Apatite	0.40	-	0.45	-	0.45	-	0.36	-
Total	100.00	21.72	100.00	26.84	100.00	27.40	100.00	23.67

Table 3. Averaged comparative DMS test data of sample no. 1 of different sizes

Size, mm	DMS products	Performance of separation, %				
		Yield	Content		Recovery	
			Fe_{total}	Fe_{magn}	Fe_{total}	Fe_{magn}
–40+10	Magnetic	50.74	29.07	19.33	67.91	83.61
	Nonmagnetic	36.00	11.43	1.37	18.94	4.20
	size – 10 mm;	13.26	21.55	10.77	13.15	12.19
	initial ore	100.00	21.72	11.73	100.00	100.00
–30+10	Magnetic	44.10	28.31	17.93	57.45	67.40
	Nonmagnetic	26.80	9.85	1.23	12.20	2.70
	size – 10 mm;	29.10	22.66	12.02	30.35	29.83
	initial ore	100.00	21.72	11.73	100.00	100.00

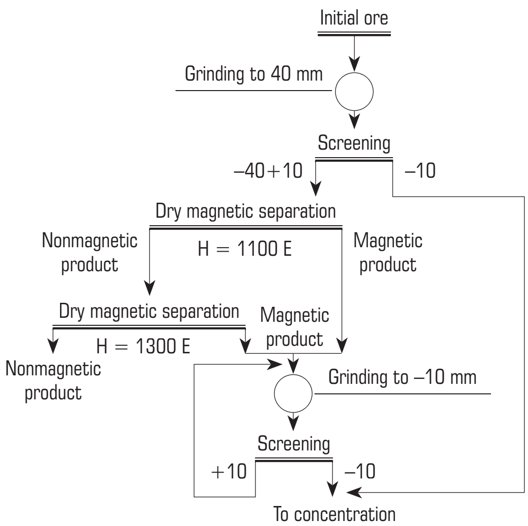

Fig. 1. Ferruginous quartzite pretreatment flowchart with DMS

Table 4. Averaged DMS test data of samples (size –40+10 mm)

Sample no.	Separation product	Performance of separation (versus initial ore), %				
		Yield	Content		Recovery	
			Fe_{total}	Fe_{magn}	Fe_{total}	Fe_{magn}
1	Magnetic	50.74	29.07	19.33	67.91	83.61
	Nonmagnetic	36.0	11.43	1.37	18.94	4.20
	size – 10 mm;	13.26	21.55	10.77	13.15	12.19
	initial ore	100.00	21.72	11.73	100.00	100.00
2	Magnetic	59.42	33.19	23.28	73.49	82.64
	Nonmagnetic	26.00	12.20	1.03	11.81	1.60
	size – 10 mm;	14.58	27.05	18.17	14.70	15.76
	initial ore	100.00	26.84	16.75	100.00	100.00
3	Magnetic	54,28	33.92	22.84	67.19	80.09
	Nonmagnetic	30,15	15.62	1.46	17.18	2.84
	size – 10 mm;	15.57	27.52	16.98	15.63	17.07
	initial ore	100.00	27.40	15.48	100.00	100.00
4	Magnetic	48.88	31.18	19.83	64.39	79.77
	Nonmagnetic	36.04	13.32	1.38	20.28	4.09
	size – 10 mm;	15.08	24.04	13.00	15.31	16.13
	initial ore	100.00	23.67	12.15	100.00	100.00

13.2 (magnetite–cummingtonite and low-metallic varieties); and the specific energy to failure can be 13.5 and 15.3 kg·m/cm^3, respectively.

So, ferruginous quartzite has a high content of low metallic and nonmetallic rocks which are removable during preparation of the raw material for processing. One of the promising ways of ferruginous quartzite pretreatment, both in Russia, in CIS countries and abroad, is the dry magnetic separation (DMS) method [6–11]. The DMS tests of the ore samples were carried in two stages at the magnetic field strength on the drum surface of 1100 E (drum speed of 40 min^{-1}) and 1300 E (drum speed 25 min^{-1}), respectively, and the magnetic and nonmagnetic products of the two stages were then united (**Fig. 1**).

The DMS performance depends on a few factors, including the most critical factor of grain size composition after grinding and screening (see Fig. 1).

Sample no. 1 was used to assess the efficiency of DMS on the sizes of –40+10 and –30+10 mm (**Table 3**). The comparison of the results shows that the content of Fe_{magn} in the nonmagnetic product changes insignificantly, which offers ground to recommend the further DMS research using the size of –40+10 mm (see Table 3).

The DMS tests of four samples –40+10 mm in size show that it is possible to reject from 26.0 to 36.0 % of low metallic and nonmetallic material with the content of Fe_{total} = 15.6–11.4% and Fe_{magn} = = 1.03–1.4%. In this case, the magnetic product of DMS gains from the increase in Fe_{total} to 29.0–33.9% and in Fe_{magn} to 19.3–22.8% (**Table 4**). The analysis of the yield of the nonmagnetic product in DMS versus the content of Fe_{magn} in the initial ore shows that DMS increases the content of Fe_{magn} by 5.5–6.1% in the magnetic product meant for the further concentration.

The mineralogy research yields that the magnetic product of DMS represents the base varieties of quartzite as follows: magnetite–hornblende (42.8–55.2%), magnetite–cummingtonite (13.4–23.2%), magnetite–garnet–amphibole (13.0–19.4%), smaller amount of magnetite–biotite (1.7–7.8%), magnetite–pyroxene (1.8–3.8%), magnetite (2.5–4.8%) and suboxydized quartzite (0.3–4.6%). The waste rock amount is 1.1–3.2%.

The nonmagnetic product of DMS contains low metallic (17.7–23.9%) and nonmetallic (71.3–78.3%) quartzite, dykes (0.2–4.4%) and shale (1.2–2.9%). Minerals are mostly nonmetallic: silicates (73.8–80.3%) and quartz (16.1–22.8%). There is a little calcite (1.1–2.2%) and apatite (0.21–0.3%). Furthermore, it is found that the low metallic varieties of the nonmagnetic product contain submicron shots of magnetite. This is proved by the experimental re-extraction of magnetite from this product ground down to a size of –0.045 mm at the content of 83–85%: the concentrate is very poor (Fe_{total} = 57.0–59.0%) and has a low yield (0.16–0.30%). The comparison of the tests with and without DMS (sample No. 1) shows that the content of Fe_{total} in the DMS-free concentrate decreases by 0.27% while its yield grows by 0.31% (**Table 5**). In this case, when at the commercial scale, the increased yield provides no compensation of expense connected with grinding of the low metallic and nonmetallic material which makes around 1/3 of the straight ore burden. The obtained results prove the advisability of the DMS application in pretreatment of ferruginous quartzite from the test deposit.

The processing properties of ferruginous quartzite are estimated in terms of grindability and processability. The grindability criterion is assumed to be the specific lab-scale mill output of the new size grades (q) –0.071 mm (I grinding stage) and –0.045 mm (II and II grinding stages). The grindability estimate is obtained relative to iron ore from Gusevogorskoe deposit (reference) using a standard procedure.

On the basis of the material constitution, texture, structure and mineralogy of ferruginous quartzite from the test deposit, and from the preliminary experimental extraction of maximum coarse grain tailings in grinding stage I, the rod milling mechanism is chosen for the tests. The magnetic product of DMS –40+10 mm in size was re-ground to the size of –10 mm and united with the screen underflow of the size of –10 mm, which was obtained before DMS, and the united product was the feed for grinding stage I in a rod mill (see Fig. 1). The laboratory test flowchart is demonstrated in **Fig. 2**.

Then, the milled product was subjected to wet magnetic separation (WMS) described in **Table 6**.

The grinding kinetics of grinding stage I product is studied using sample No. 1. The data analysis shows that with increasing grinding time, the yield of the sizes of –0.071 and –0.045 mm noticeably grows, and the specific mill output *q* decreases as the concentrate yield does, while the quality of the concentrate improves (see Table 6). The content of Fe_{magn} in the tailings of WMS is unchanged (0.84–0.90%). The relative grindability of quartzite as against the reference is 1.92 times higher.

It is found that the relative grindability coefficient K_{grind} of Okolovo ferruginous quartzite exceeds the reference: by 1.09 times in stage II and by 1.05 times in stage III (**Table 7**). Grinding of quartzite in stage I down to the size of –0.071 mm at the content of 23.8–31.2% produced the concentrate at the yield from 28.33 to 44.9 % (relative to the prime concentrate) at the content of Fe_{total} = 41.9–49.3%. The tailings contained Fe_{total} = 12.7–14.6% and Fe_{magn} = 0.48–0.94%.

The grindability tests in stages II and III were performed in a ball mill, re-grinding of stage III concentrate was aimed to produce a high-quality concentrate (at the content of Fe_{total} not less than 70%) [12–17]. In this manner, the yield of coarse tailings in stage I varies from 29.1 to 35.6% (relative to initial), and, considering the earlier tailings of DMS, the yield of waste increase to 60%. In the tailings of WMS stage I, the yield of the coarse sizes (+0.16 mm) in the test samples varies from 27.7 (sample no. 4) to 36.4% (sample No. 1), which offers ground to recommend this waste as a coarse-grained building material.

From the concentrates of stage I, after re-grinding to the size of –0.045 mm at the content of 62.4–68.9% and after wet magnetic separation, the resultant two-circuit concentrate has Fe_{total} = = 68.1–69.5% at the yield of 51.6–62.2% (per circuit) and the tailings have Fe_{total} = 13.8–16.4% and Fe_{magn} = 0.36–0.84%.

From the concentrates of stage II, after re-grinding to the size of –0.045 mm at the content of 80.9–84.9% and after wet magnetic separation, the resultant concentrate had the content of $Fe_{total} \geq 70.0$ (70.3–70.73%)% with the external specific surface of 2200 cm^2/g. It should be mentioned that despite a comparatively low content of the size –0.045 mm, the concentrates mostly contain free metallic grains (95.0–97.0%), and the dissociation of the metallic phase in stage III

Table 5. Averaged comparative test data of sample no. 1 with and without DMS

Separation product	Performance of separation (versus initial ore), %					
	Without DMS			With DMS		
	Yield	Content of $Fe_{total/magn}$	Recovery of $Fe_{total/magn}$	Yield	Content of $Fe_{total/magn}$	Recovery of $Fe_{total/magn}$
Concentrate	16.36	70.07/67.45	52.78/94.00	16.05.22	70.30/67.75	51.95/92.70
Nonmagnetic product	–	–	–	36.00	11.43/1.37	18.95/4.19
Wet separation tailings	83.64	12.21/0.84	47.22/6.00	47.95	13.18/0.84	29.10/3.11
Initial ore	100.00	21.72/11.73	100.00	100	21.72/11.73	100.00

Table 6. Averaged testing data (grinding+concentration) of sample no. 1

Grinding time, min	Performance of separation (versus initial ore), %				
	Content of size grade 0.071/0.045 mm in ground product, %	Separation products	Yield	Content of $Fe_{total/magn}$	q in size grade 0.071/0.045 mm, kg/(l·h)
3	24.7/12.1	Concentrate Tailings Initial ore	50.45 49.55 100.00	42.00/- 12.76/0.94 27.51/17.60	0.484/0.209
7	31.7/20.5	Concentrate Tailings Initial ore	47.53 52.47 100.00	44.45/- 13.32/0.85 27.51/17.56	0.301/0.202
15	47.4/25.3	Concentrate Tailings Initial ore	34.84 65.16 100.00	53.13/- 13.81/0.94 27.51/17.56	0.238/0.124
23	61.2/34.5	Concentrate Tailings Initial ore	32.86 67.14 100.00	56.07/- 13.53/0.85 27.51/17.56	0.211/0.118

Table 7. Averaged test data of samples per grinding stages

Sample no.	Grinding stage I			Grinding stage II			Grinding stage III		
	Specific output of newly formed size grade, q, kg/(l·h)								
	Initial feed	Size grade –2/–0.071 mm	K_{grind}	Initial feed	Size grade –0.045 mm	K_{grind}	Initial feed	Size grade –0.045 mm	K_{grind}
1	2.68	1.57/0.47	2.03	0.324	0.208	1.01	0.680	0.209	1.07
2	2.34	1.44/0.49	1.87	0.480	0.248	1.20	0.906	0.181	0.92
3	2.08	1.44/0.46	1.87	0.400	0.220	1.07	0.680	0.226	1.15
4	1.44	0.92/0.34	1.19	0.480	0.245	1.19	0.618	0.233	1.19
Average	2.36	1.48/0.48	1.92	0.4010	0.225	1.09	0.755	0.205	1.05

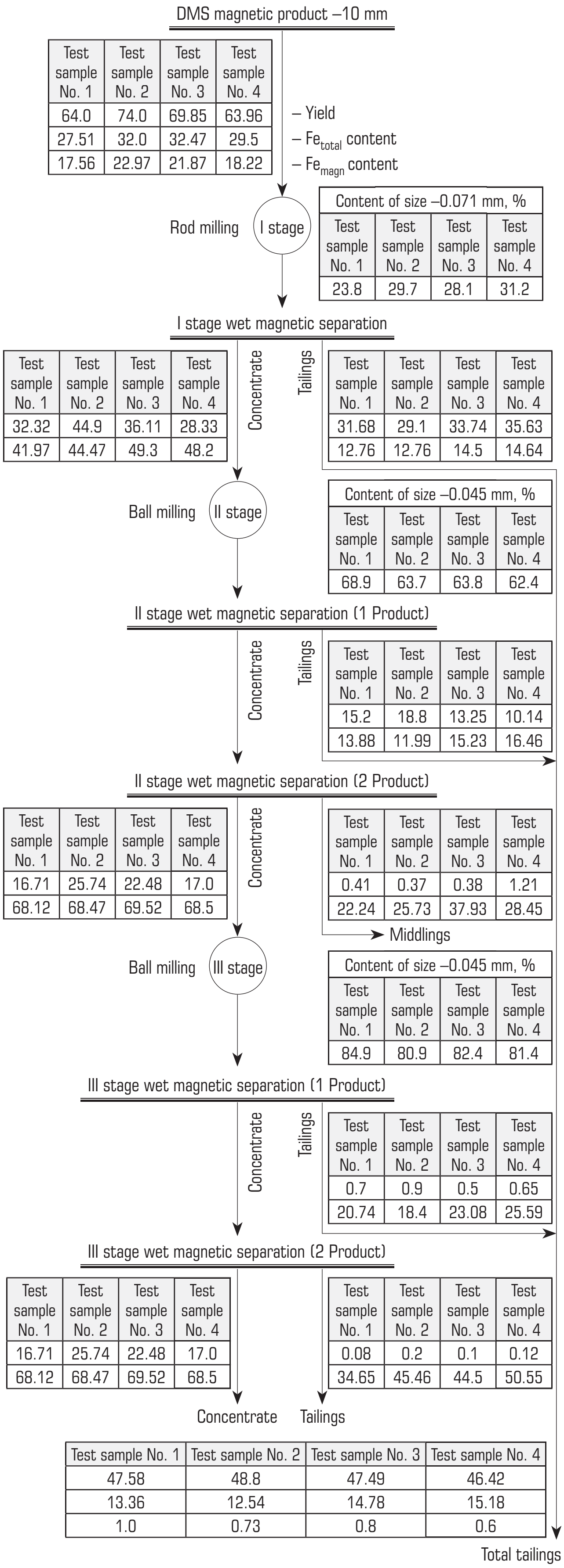

Fig. 2. Lab-scale processability test flowchart

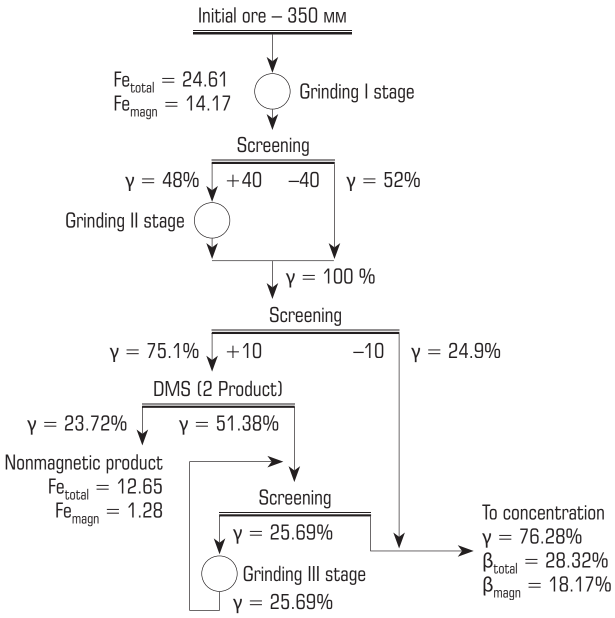

Fig. 3. Recommended pretreatment flowchart

concentrate was 0.98–0.99 in all test samples. After WMS stage I, the concentrate already contains from 28.0 to 41.5% of free metallic grains which, after re-grinding in stages II and III, acquire the larger external specific surface. Removal of the free metallic grains from the process can reduce the loss of magnetite owing to recommended fine screening, which can increase the yield of the concentrate and cut down the milling cost. The granulometry of stage III concentrate in all test samples shows that the highest quality size grade is –0.045 mm and the lowest quality size grade is +0.071 mm.

The full flowchart of the processing property studies of the test samples is given in Fig. 2.

With a view to assessing further improvability of the concentrate quality, sample No. 1 was subjected to stage IV of grinding to the size of –0.045 mm at the content of 94.2% and to subsequent separation. The resultant concentrate was overground (the external specific surface increased to 2340 cm^2/g) and had the content of $Fe_{total} = 70.9\%$. However, the larger external specific surface will later on complicate filtration of such concentrate.

The obtained results were then checked in the larger scale tests on a continuous-operation plant, which made it possible to develop and recommend the pretreatment and overall processing flowcharts for ferruginous quartzite of Okolovo deposit (**Figs. 3** and **4**).

The mathematical processing of the larger-scale laboratory test data produced the empirical dependences of the content of Fe_{total} in the concentrate on the content of –0.045 mm size in each test sample (**Fig. 5**). The variation in the curves in Fig. 5 is governed by the size of magnetite shots and by the hardness of the test rocks.

Conclusions

1. Based on the grade analysis of magnetite grains and aggregates, the test ferruginous quartzite is estimated as medium-impregnated rock (average size is –0.0662 mm).

2. Regarding physical and mechanical properties, the test quartzite has low hardness (hardness factor on Protodyakonov's scale is

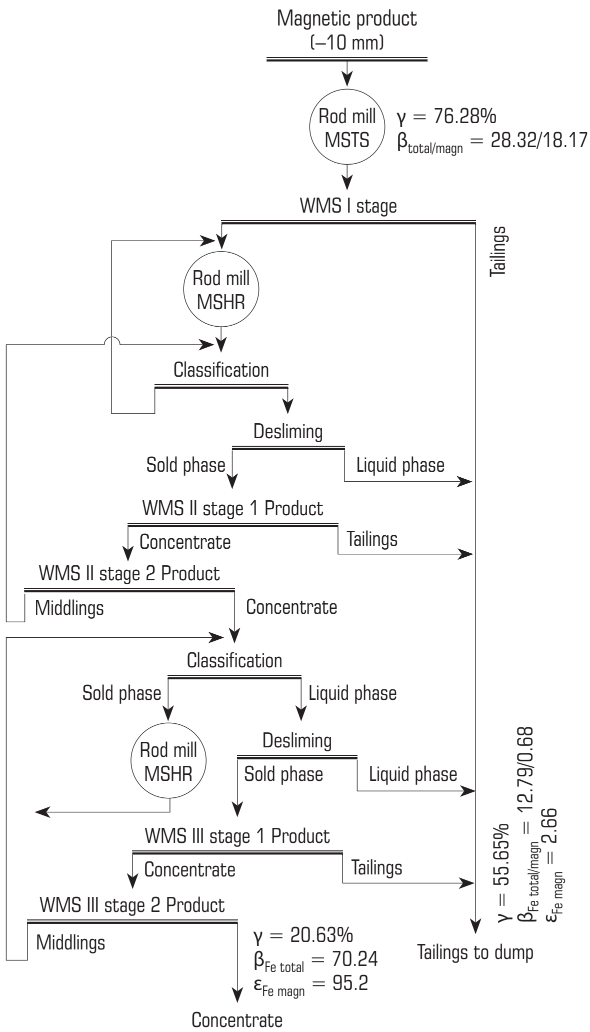

Fig. 4. Recommended processing flowchart for ferruginous quartzite of test deposit

5.31–6.12; specific energy to failure is 4.0–5.06 kg m/cm^3). The average grindability coefficients per grinding stages are: I—1.92; II—1.09 and III—1.05.

3. It should be highlighted that because of very much low metallic and nonmetallic material present in the ferruginous quartzite, the yield of tailings is high, and the tailings require further treatment.

4. Regarding processability, the ferruginous quartzite of the test deposit is an easy mineral, and magnetite exhibits higher susceptibility to overgrinding.

5. The recommended processing technology for the test ferruginous quartzite allows production of the high-quality magnetite concentrate suitable for the further metallization: Fe_{total} = 70.24%; yield 20.63%; recovery of Fe_{magn} 95.2%.

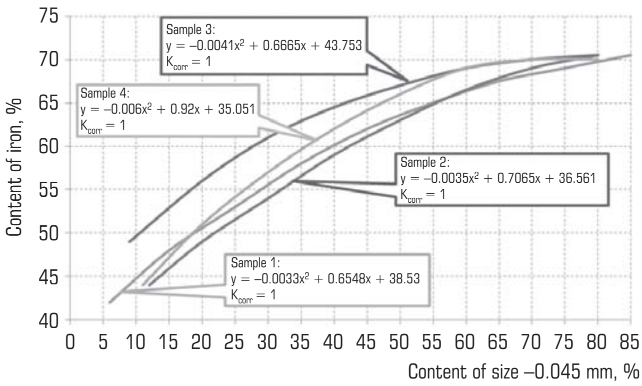

Fig. 5. Effect of grinding coarseness on Fe_{total} content in concentrate

References

1. Solodilova V. V. Geological and structural features of the Okolovsky deposit of ferruginous quartzites. *Lithosphere*. 2006. No. 1(24). pp. 45–55.
2. Selivanova E. V. The possibility of complex use of ores of the Okolovsky deposit of iron quartzites. *Metallogeny of ancient and modern oceans*. 2008. No. 1. pp. 135–138.
3. Gzogyan T. N. Special features of the Prioskolskoye deposit ferruginous quartzites material composition and processing technology. *Obogashchenie Rud*. 2010. No. 2. pp. 8–12.
4. Gzogyan T. N., Gzogyan S. R. Ferruginous quartzites from Kimkan deposit and their processing. *Journal of Mining Science.* 2017. Vol. 53, No. 1. pp. 149–157.
5. Baoyu Cui, Dezhou Wei, Hao Zhang. et al. Beneficiaton studies of a low-grade iron ore in China. *In: XXVIII International Mineral Processing Congress (IMPC). Quebec, Canada*. 2016. 120.
6. Lu L. Iron Ore: Mineralogy, Processing and Environmental Sustainability. Cambridge : Woodhead Publishing, 2015. 631 p.
7. Chanturia V. A. Innovation-based processes of integrated and high-level processing of natural minerals and mining waste. *Gornyi Zhurnal*. 2015. No. 7. pp. 29–37.
8. Varichev A. V., Ugarov A. A., Efendiev N. T., Kretov S. I., Puzakov P. V. et al. Innovative solutions in iron ore production at Mikhailovsky mining and processing plant. *Journal of Mining Science.* 2017. No. 5. pp. 141–153.
9. Gleeson D. Preceding processing. *International Mining*. 2019. pp. 82–87.
10. Yu J. W., Han Y. X., Li Y. J. et al. Investigation on pre-concentration efficiency of a low grade hematite ore using magnetic separation. *XXVIII International Mineral Processing Congress (IMPC).* Quebec, Canada. 2016. 34.
11. Kuskov V. P., Sishchuk Yu. M. Improvement of beneficiation technologies foe iron ore of various type and material constitution. *Gornyi Zhurnal*. 2016. No. 2. pp. 70–73.
12. Gzogyan T. N. Theoretical and experimental studies on production of high grade concentrates. *GIAB*. 2010. No. 4. pp. 389–394.
13. Papalambros P. Y., Wilde D. J. Principles of optimal design: modeling and computation. New York : Cambridge University Press, 2017. 376 p.
14. Pelevin A. E. Production of hematite concentrate from hematite-magnetite ore. *GIAB*. 2020. No. 3(1). pp. 422–430.
15. Opalev A. S., Khokhulya M. S., Fomin A. V. et al. Creation of innovative technologies for production of high-quality iron concentrate production in the North West of Russia. *Gornyi Zhurnal*. 2019. No. 6. pp. 56–60.
16. Dyadin B. I. Electrodynamic separation of fine particles in the pulsed traveling magnetic field. *Journal of Mining Science.* 2020. Vol. 56, No. 1. pp. 113–118.
17. Gan F., Peng X., Yang B. Study on process for recovering iron concentrate from iron-containing solid waste in mines. *Journal of Mining Science.* 2020. Vol. 56, No. 4. pp. 669–677.